Selective transport of Zn^{2+} through liquid and solid membranes containing pyrazole-tetrazole hybrid carriers

Tarik Harit[a], Mounir Cherfi[a], Smail Triki[b], Mohamed Khayet[c,d], Fouad Malek[a],*

[a] Laboratory of Applied Chemistry and Environment -ECOMP, Faculty of Sciences, Mohamed 1st University, Bd Mohamed VI, BP: 717, Oujda, 60000, Morocco.

[b] Univ Brest, CNRS, CEMCA, 6 Avenue Victor Le Gorgeu, C.S. 93837 - 29238 Brest Cedex 3, France

[c] Department of Structure of Matter, Thermal Physics and Electronics, Faculty of Physics, University Complutense of Madrid, Avda. Complutense s/n, 28040 Madrid, Spain

[d] Madrid Institute for Advanced Studies of Water (IMDEA Water Institute), Avda. Punto Com N◦ 2, 28805 Alcalá de Henares, Madrid, Spain

*Corresponding author: Tel.: +212 536 500601, Fax: +212 536 500603, E-mail Address: fouad_malek@yahoo.fr; f.malek@ump.ac.ma (Fouad Malek)

Abstract

Both liquid ($\mathbf{M_L}$) and solid ($\mathbf{M_S}$) membranes bearing a pyrazole-tetrazole hybrid molecule as carrier are developed. The $\mathbf{M_L}$ membrane is composed of CH_2Cl_2 solution inserted between an aqueous solution of metal nitrate, as a source phase, and a receiving phase containing deionized water. The $\mathbf{M_S}$ membrane was prepared by photopolymerisation of pyrazole-tetrazole monomer and a polyacrylonitrile support. Being thermally stable up to 330ºC, the $\mathbf{M_S}$ membrane exhibits an asymmetric amorphous structureIt was found that both membranes selectively transport Zn^{2+} over Cu^{2+}, Pb^{2+}, Cd^{2+}, and Co^{2+} cations. At 25ºC and neutral pH, the permeate flux of Zn^{2+} reached 6.1 10^{-4} $mol.h^{-1}.m^{-2}$ for the $\mathbf{M_L}$ membrane and 1.88 10^{-2} $mol.h^{-1}.m^{-2}$ for the $\mathbf{M_S}$ membrane. Although the $\mathbf{M_S}$ membrane exhibits more efficient Zn^{2+} permeate flux and higher stability than those of the $\mathbf{M_L}$ membrane, the selectivity to Zn^{2+} transport of the $\mathbf{M_S}$ membrane was found to be lower.

Keywords: Facilitated transport; Liquid Membrane; Pyrazole-tetrazole; Solid membrane; Zinc cation, transition metal ions

1. Introduction

Zinc plays an important role in different fields, especially in medicinal chemistry [1]. It is used in a variety of pharmaceutical products and applications as antimicrobial [2], anticancer [3], and antiviral [4] agent as well as in the treatment for Alzheimer's disease [5]. More recently, zinc has been studied as a potential treatment for COVID-19 [6,7]. Being an essential nutrient that plays a critical role in the functioning of the immune system, some studies have suggested that zinc supplementation may help to reduce the severity of COVID-19 symptoms. Research suggests that zinc ions can interfere with the replication of the virus and thus may help to decrease the duration of symptoms and the risk of complications from the disease. Furthermore, zinc is reported to be a cofactor of many enzymes and its presence is essential for the proper functioning of many biochemical pathways [8]. In this context, the price of this metal had more than doubled during the period from April 2020 to April 2022 [9]. Therefore, the recovery of this metal, especially from aqueous media becomes crucial. In fact, this will not only ensure conserving resources but also helps in reducing environmental pollution.

The separation of Zn^{2+} metal ions is achieved through various methods, including liquid-liquid [10] and solid-liquid [11] extractions. However, such methods are considered as batch processes and require their regeneration after each cycle, limiting significantly their performance and ability to extract zinc ions over time. Compared to these traditional separation methods, tmembrane technologies offer several advantages such as a continuous process, treatment of sensitive substances under mild conditions, energy savings and a solution to environmental regulation requirements [12]. According to Grand View Research, the global market for membrane separation technologies reached $24.65 billion in 2022 and is expected to grow to $62.5 billion by 2030 [13].

It is worth quoting that some membranes bearing pyrazolic transporters were developed for the selective separation of metal cations such as cesium [14], potassium [15], lithium [16] and cadmium [17]. Other membranes bearing tetrazole derivatives were tailored for different selective separations including ultrafiltration (UF) [18], C_2H_2/CO_2 and C_2H_2/C_2H_4 separation [19]. Furthermore, some membranes were designed including tetrapods [20] macrocycles [21] and linear structures [22]. Therefore, it will be very interesting to explore their ionophore properties to play the role of carrier for the selective separation of Zn^{2+} via liquid and solid membranes. In the present study, both liquid and solid membranes bearing pyrazole-tetrazole carrier are proposed for the selective transport of Zn^{2+} cation.

2. Materials and methods

2.1 *Materials and characterization techniques*

Reagent-grade chemicals and solvents were obtained from Sigma-Aldrich and used as received. The 1H NMR analysis was performed at 500 MHz using BRÜKER AC spectrometer. Chemical shifts (δ) are reported in parts per million (ppm) relative to the residual peak of the $CDCl_3$ solvent (7.27 ppm). The multiplicity is indicated as s = singlet, d = doublet, t = triplet, q = quartet, m = multiplet. Mass spectra were acquired using a Platform II Micromass instrument (ESI+, CH_3CN/H_2O: 50/50). Perkin Elmer 240C Elemental Analyzer was used to carry out the elemental analysis. TGA Q50 (TA instrument) analysis was carried out by heating 10 mg of membrane sample from 25°C to 500°C maintaining the heating rate at 10 °C.min^{-1}. Scanning electron microscopy (SEM) images and energy-dispersive X-ray spectroscopy (EDS) analysis were conducted using a HIROX SH-5500P microscope coupled to the detector. Methyl 1-((2-(3-propyl)-2H-tetrazol-5-yl)methyl)-5-methyl-1H-pyrazole-3-carboxylate **1** and (5-methyl-1-

((2-propyl-2H-tetrazol-5-yl)methyl)-1H-pyrazol-3-yl)methanol **2** were synthesized according to the procedure previously described our research group [20].

2.2 *Synthesis procedure*

2.2.1 Synthesis of monomer 5-methyl-1-((2-propyl-2H-tetrazol-5-yl)methyl)-1H-pyrazol-3-yl)methyl acrylate (monomer 3)

Acrylic acid ($0.47\ 10^{-3}$ mol) was slowly added to a mixture of (5-methyl-1-((2-propyl-2H-tetrazol-5-yl)methyl)-1H-pyrazol-3-yl)methanol **2** ($0.4\ 10^{-3}$ mol), dicyclocarbodiimide ($0.4\ 10^{-3}$ mol) and 4-Dimethylaminopyridine (DMAP) (0,05g) in 25 mL of methylene chloride cooled to 0 °C. The resulting mixture was stirred at room temperature for 24 hours. The obtained solid residue was filtered, and the filtrate was then concentrated under reduced pressure at 30 °C. The monomer was purified through a silica column (Ether/EtOH ; 98/2 ; $R_f = 0.23$) to get 5-methyl-1-((2-propyl-2H-tetrazol-5-yl)methyl)-1H-pyrazol-3-yl)methyl acrylate **3** in 83% yield as colorless oil: ^{1}H NMR ($CDCl_3$, 200 MHz): 0.82 (t, J = 7.4 Hz, 3H, $C\underline{H}_3$-CH_2); 1.86 (m, J= 7.2 Hz, 2H, CH_3-$C\underline{H}_2$); 2.32 (s, 3H, $C\underline{H}_3$-Pz); 3.69 (t, J= 7.1 Hz, 2H, $C\underline{H}_2$-NTz); 5.41 (s, 2H, Tz-$C\underline{H}_2$-Pz); 5.85 (m, 1H, $\underline{H}$-CH=C-CO); 6.09 (s, 1H, $\underline{H}$Pz); 6.22 (s, 1H, CH_2=C$\underline{H}$-CO); 6.40 (m, 1H, $\underline{H}$-CH=C-CO). MS (ESI): m/z = 291.1 $[M+H]^+$. Anal. Calcd for $C_{13}H_{18}O_2N_6$ (**3**):C, 53.78; H, 6.25; N, 28.95 Found: C, 53.92; H, 6.42; N, 29.13.

2.2.2 Synthesis of the solid membrane (M_S)

The monomer **3** (0.13 g; 0.2 mmol), styrene (0.11 g; 1.05 mmol), 1,4-divinylbenzene (0.013 g; 0.1 mmol) and 2,2-dimethoxy-2-phenylacetophenone (5.2 mg; 0.02 mmol) were mixed in a test tube. The mixture was then stirred for 5 min at room temperature and then cast on a flat polyacrylonitrile (PAN) support (2x2 cm^2) (PAN Carbone Lorraine, MWCO 50 000) using a threaded hand-coater rod to form an uniform layer with 6 µm thickness followed by an

exposition to UV radiation via a mercury vapor lamp (250-440 nm) from a Silair device, for 30 s at room temperature.

2.3. Extraction experiments

Extraction experiments in competitive (i.e., all metal cations are present in the solution) and non-competitive conditions together with the back-extraction experiment were performed according to the procedures reported elsewhere [14]. The following equation was used to calculate the extraction percentage *E* (%):

$$\boldsymbol{E\ (\%) = \frac{C_o - C}{C_o} \times 100} \qquad \textbf{(1)}$$

where C_0 and C are the initial metal concentration and the metal concentration at the equilibrium, respectively. All experiments were performed in triplicate.

2.4 *Transport experiments*

2.4.1 Transport experiments through liquid membrane

The liquid membrane transport (Fig. 1) consists on two different experiments, the no-competitive and competitive conditions:

(i) for the non-competitive conditions, the source phase is an aqueous solution (10 mL) of metal nitrate (10^{-3} M), the liquid membrane is composed by CH_2Cl_2 solution (40 mL) of **2** ($7\ 10^{-5}$ M), and the receiving phase is deionized water (20 mL).

(ii) for the competitive conditions, the source phase is an aqueous solution (10 mL) containing the five-metal nitrate with a similar fixed concentration ($2\ 10^{-4}$ M), while the membrane and the receiving phases are similar to those used for the non-competitive conditions.

The organic phase was continuously stirred at 200 rpm and the concentration of the metallic cations was obtained by atomic absorption technique. The effective area "*S*" of the membrane

with the two aqueous phases is $S = \pi \times 10^{-4}$ m^2. All experiments were conducted in triplicate at room temperature (25 °C).

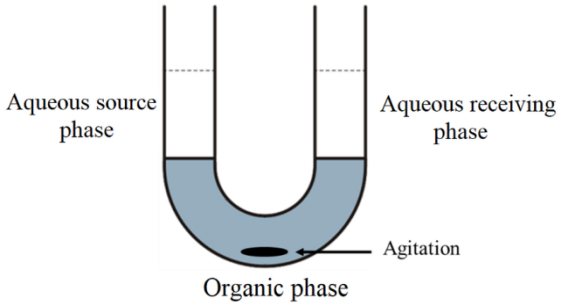

Fig. 1. Experimental set-up used for the transport through the liquid membrane.

2.4.2 Transport experiments through solid membrane

The experimental set-up employed to conduct transport experiments through the prepared solid membrane **Ms** is depicted in Fig. 2.

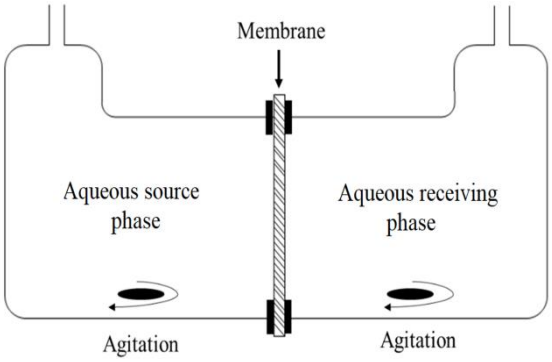

Fig. 2. Experimental set-up used for the transport through the solid membrane.

The set-up consists of two half-cells, each with a 75 mL capacity, representing the source and receiving aqueous phases, separated by the polymeric membrane. The aqueous phases were stirred at 200 rpm. The membrane's surface area in contact with the two phases is 7.07 x 10^{-4} m^2. In the simple mode, where the receiving phase contains only deionized water, the feeding

phase contains 10^{-3} M metal nitrate solution under non-competitive conditions, while for the competitive transport, a concentration of 2×10^{-4} M was used for each metal salt. In the against-protons current mode, the receiving phase contains a nitric acid solution of 2×10^{-3} M solution. All experiments were carried out in triplicate at 25°C.

2.4.3. Flux (*F*) and selectivity (*S*) calculations

The experiments were carried out over a sufficiently long time (12 h) to be able to calculate the diffusion flux (*F)* and the selectivity (*S),* using the two following equations:

$$F = \rho V/A \quad (2)$$

$$S = F_{Zn}^{2+} / F_{M}^{2+} \quad (3)$$

where, *F, S, ρ, V* and *A* are the diffusion flux (mol h^{-1} m^{-2}), the selectivity, the slope of the curve: $C_{M2+} = f(t)$ (mol L^{-1} h^{-1}), the volume of the reception phase and the area of the membrane in contact with the two aqueous phases.

2.4.4 Membranes stability test

The stability of both liquid and solid membranes together with their reusability were evaluated by conducting repeated competitive transport experiments using the same membranes for 8 cycles of 12 h each. This was performed by renewing both the source and the receiving solutions after each experiment.

3. Results and discussion

3.1 *Synthesis*

3.1.1. Synthesis of the monomer 5-methyl-1-((2-propyl-2H-tetrazol-5-yl)methyl)-1H-pyrazol-3-yl)methyl acrylate (monomer 3)

The first step was to convert the ester compound **1** to the corresponding alcohol **2**. The compound **2** can be attached to a polymer support either by grafting to a functionalized polymer or by attaching polymerizable double bonds. Since the first method results in very low grafting rates that could reduce the performance of the membranes, the second method was followed in this study. The compound **2** has a hydroxyl group on its side arm. This allows its functionalization by an acrylic double bond, which is highly reactive in the polymerisation process (Fig. 3).

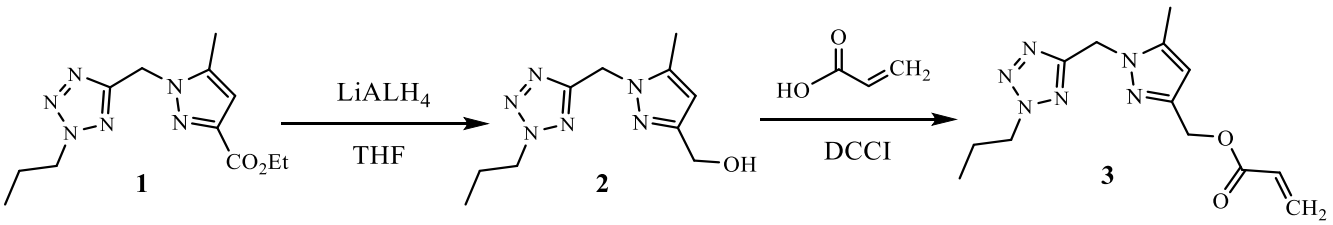

Fig. 3. Followed pathway for the synthesis of monomer **3.**

The synthesized monomer **3** exhibits a good yield (75 %) and its structure was confirmed by spectroscopic and spectrometric analyses.

3.1.2 Preparation and characterization of Ms membrane

The Ms membrane was prepared by means of the photo-polymerization of the formulation containing monomer **3** [14]. As it is well known, the diffusion flux of species across a membrane is inversely proportional to the membrane thickness [23]. However, a thin membrane is expected to be less mechanically stable and consequently requires its casting on solid support [14]. In this context, in this study PAN was selected as support because of its exceptional mechanical properties [24], high ion diffusion rates and high porosity or void volume fraction [25].

The SEM top surface and cross-section images of the prepared Ms membrane are presented in Fig. 4. As can be seen Ms is a composite membrane formed by a dense top layer formed on a porous PAN containing finger-like structure. This membrane morphological structure together

with its amorphous character could improve the diffusion of cations across the membrane as claimed by Gherrou et al. [26], who observed that a membrane with a high concentration of a crown ether carrier results in the crystallization of the film by formation of multilayers, precluding significant flux diffusion of the studied metal ions. Both the membrane and the PAN support were subjected to Energy-dispersive X-ray spectroscopy (EDS) analysis. The obtained spectra are depicted in **Fig. S1** and their qualitative elementary composition is summarized in Table 1. Compared to the PAN support, the **Ms** membrane shows a drop in the amount of carbon (*ca.* 4 %) with an increase of that of oxygen (*ca.* 12 %). This is expected given the nature of the reagents grafted on the active layer of the **Ms** membrane. The oxygen detected in PAN, estimated as 3.88 %, may be attributed to the initiator used to synthesize this polymer or to the moisture present within this support.

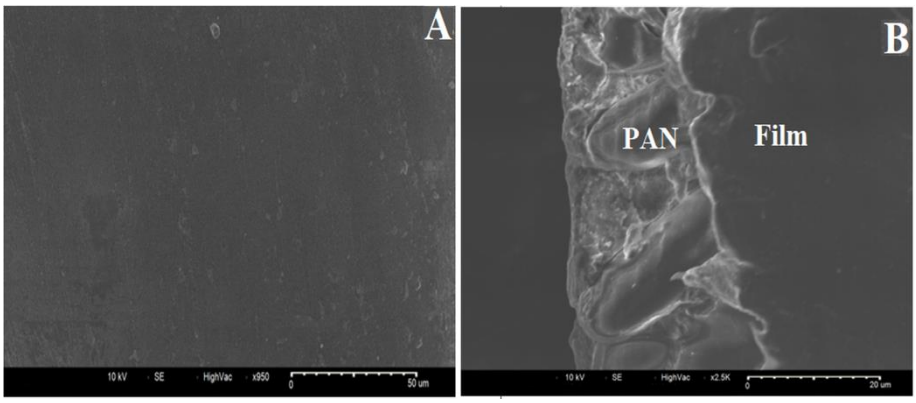

Fig. 4. SEM images of the top (A) and cross-section (B) of the Ms membrane.

Table 1. Elemental composition of the PAN and the solid **Ms** membrane.

	PAN	**Ms**
%C	84.59	80.52
%O	3.88	16.08

202 The thermal properties of the membrane **Ms** and the PAN support were studied through TGA
203 test. As shown in Fig. 5, for the PAN support an initial weight loss of 15 % was detected in the
204 range of 20-100 °C. This is associated with the moisture loss and/or solvent present in the
205 sample. A second loss of 4% by weight observed in the range 290-330 °C, can be attributed to
206 dehydrogenation reactions and the release of volatile compounds [27,28]. Then, the PAN starts
207 to degrade with increasing temperature above 330ºC. At 450 °C a weight loss of approximately
208 60% was registered. At this temperature, the PAN partially carbonizes. The deposition of the
209 active layer on the PAN support, Ms membrane, improves the thermal stability up to 330 °C.
210 The membrane only loses around 6 % of its weight between 100 and 300 °C. This weight loss
211 presumably corresponds to the loss of moisture. For a further temperature increase, a weight
212 loss of 75 % was observed due to the degradation of the various fragments grafted onto the
213 macromolecular chains. These findings show that the prepared membrane exhibits good
214 thermal stability.

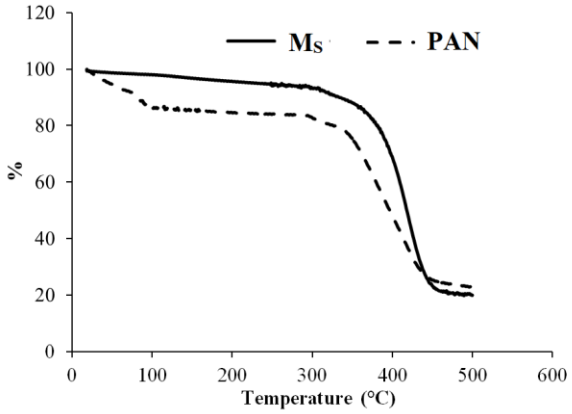

215

216 **Fig. 5.** Thermogravimetric analysis (TGA) curves of the membrane **Ms** and the PAN support.

217 3.2 *Liquid–liquid extraction*

218

219 Prior to investigating the transport of transition metal ions Zn^{2+}, Cu^{2+}, Pb^{2+}, Cd^{2+} and
220 Co^{2+} through the synthesized membranes, we conducted an assessment of the ability of

compounds **1** and **2** to extract these cation metals using the individual liquid-liquid extraction method. During this extraction process, the nitrate anion was chosen as counter-ion. The obtained results summarized in Table 2, reveal clearly that both compounds **1** and **2** have no significant affinity towards Cd^{2+} and Co^{2+} metal ions, while they show affinity to extract Zn^{2+} and Cu^{2+}, with a much more significant preference for Zn^{2+} metal ion.

Table 2. Yields of extraction of individual cations by compounds **1** and **2.**

Ligand	**Zn^{2+}**	**Cu^{2+}**	**Pb^{2+}**	**Cd^{2+}**	**Co^{2+}**
1	62±2	17±2	7±1	0	0
2	25±1	9±2	8±1	0	0

In addition, it was observed a decrease of the extraction efficiency when the ester compound **1** was converted to its corresponding alcohol **2**. This could be attributed to the presence of the hydroxyl group that increases the hydrophilic character of compound **2** and consequently the loss of the extractor in the aqueous phase. The extraction selectivity is determined in the simultaneous presence of all transition metal ions at equal concentration in the aqueous phase. The resulting data are summarized in Table 3.

Table 3. Yields of competitive extraction of metal cations in presence of compounds **1** and **2.**

Ligand	**Zn^{2+}**	**Cu^{2+}**	**Pb^{2+}**	**Co^{2+}**	**Cd^{2+}**
1	38±2	7±1	2±1	0	0
$S_{Zn^{2+}/M^{2+}}$	---	5.4	19	---	---
2	10±3	4±1	1±2	0	0
$S_{Zn^{2+}/M^{2+}}$	---	2.5	10	---	---

The first remark to be drawn is the decrease of the percentage of extraction maintaining the order $Zn^{2+} > Cu^{2+} > Co^{2+} \approx Pb^{2+} \approx Cd^{2+}$. This could be attributed to the simultaneous presence

of all cations in the aqueous phase. In contrast the selectivity $S_{Zn^{2+}/M^{2+}}$ showed a significant enhancement. The competitive extraction results, specifically the Zn^{2+}/ Cu^{2+}, Cu^{2+}/ Pb^{2+}, selectivity ratios, indicate the strong propensity of compounds **1** and **2** for preferentially binding with Zinc cation.

The decomplexing process (i.e., back-extraction) of the transition metal cation from its complex was investigated by adding the complex (Compound **1** / cation) present in the organic phase to pure water. As shown in Table 4, over half of the fraction of heavy cations, which had been complexed within the compound **1**, was released into the aqueous phase. This outcome aligns with the objective of selectively transporting the Zn^{2+} ions.

Table 4. Yields of back-extraction of metal cation extracted with compound **1.**

Cations	Back-extraction percentage %
Zn^{2+}	43±3
Cu^{2+}	56±1
Pb^{2+}	58±2

3.3 *Facilitated transport of transition metal cations across the liquid membrane* M_L

The transport of transition metal cations (Cu^{2+}, Zn^{2+}, Co^{2+}, Pb^{2+} and Cd^{2+}) has been investigated both individually and competitively. Table 5 summarizes the diffusion flux (F) and the $F_{Zn^{2+}}$/ $F_{M^{2+}}$ selectivity values.

Table 5. Diffusion flux (10^{-4} mol h^{-1} m^{-2}) and $F_{Zn^{2+}}$/ $F_{M^{2+}}$ selectivity through the liquid membrane $\mathbf{M_L}$.

$F_{M^{2+}}$ and $F_{Zn^{2+}}$/ $F_{M^{2+}}$	Individual Transport	Competitive Transport
$F_{Zn^{2+}}$	15.0±0.4	6.1±0.2
$F_{Cu^{2+}}$	7.1±0.2	1.7±0.3
$F_{Pb^{2+}}$	4.3±0.5	0.8±0.1

F_{Cd}^{2+}	0.0	0.0
F_{Co}^{2+}	0.0	0.0
F_{Zn}^{2+}/F_{Cu}^{2+}	2.1	3.6
F_{Zn}^{2+}/F_{Pb}^{2+}	3.5	7.6

The obtained results of the individual transport mode are also displayed in Fig. 6A, as the variation of cation concentration of each metal ion (Zn^{2+}, Cu^{2+}, Pb^{2+}, Cd^{2+}, Co^{2+}) *versus* time. In addition to the perfect linear variation for all metal ions, this study reveals clearly that the transport of Zn^{2+} is faster than those observed for the other metal ions. The diffusion flux of Zn^{2+} is 15×10^{-4} mol.h^{-1}.m^{-2}, whereas those of Cu^{2+}, Pb^{2+}cations are 7.1×10^{-4} and 4.3×10^{-4} mol.h^{-1}.m^{-2}, respectively. Indeed, the Zn^{2+} flux is at least 2.1 times higher than that of the other cations, indicating that the developed M_L membrane exhibits better Zn^{2+} transport than the other cations. This result aligns with those obtained during extraction experiments performed with compounds **1** and **2** evidencing that the ionophore properties of both compounds were kept inside the membrane. The present findings are supported by monitoring the evolution of the concentrations in the receiving phase during the study of competitive transport of the five metal ions simultaneously. The source phase contains the five metal ions at an equal concentration of 2×10^{-4} M (Fig. 6B). The diffusion flux of Zn^{2+} was found to be 6.1×10^{-4} mol.h^{-1}.m^{-2}, whereas that of $Cu^{2+}$and Pb^{2+} are only 1.7×10^{-4}, and 0.8×10^{-4} mol.h^{-1}.m^{-2}, respectively. As it was expected from results obtained during the extraction experiments, the $Co^{2+}$and Cd^{2+} diffusion fluxes were null. The transport selectivity of the zinc cation compared to copper and lead cations are 6.1 and 1.7, respectively. This proves that the $\mathbf{M_L}$ membrane transports selectively the zinc cation.

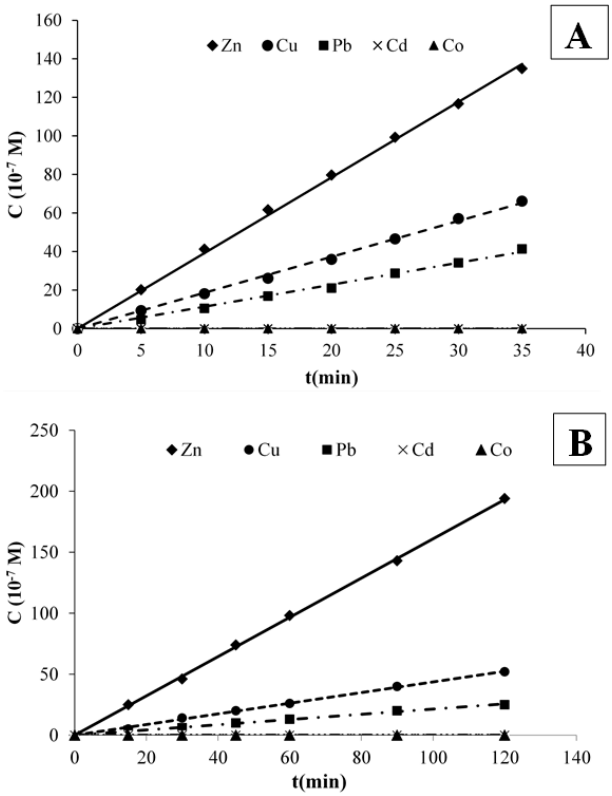

Fig. 6. Individual (A) and competitive (B) transport of transition cations through the **M**$_L$ liquid membrane and temporal evolution of the concentrations of each ion in the reception phase.

3.4 *Facilitated transport of metal transition cations across the solid membrane M*$_S$

The diffusion of transition metals from the source phase to the receiving phase is also achieved through the prepared solid membrane **M**s. The temporal evolution of concentrations in individual mode is depicted in Figure 7 and the diffusion flux (*F*) and selectivity (*S*) values are summarized in Table 6.

Table 6. Flux diffusion (10^{-3} mol h^{-1} m^{-2}) and $F_{Zn^{2+}}/F_{M^{2+}}$ selectivity through the solid membrane **M**S.

$F_{M^{2+}}$ and $F_{Zn^{2+}}/F_{M^{2+}}$	Individual transport	Competitive transport	Competitive transport against proton current
$F_{Zn^{2+}}$	24.7±0.3	18.8±0.6	72.5±0.8
$F_{Cu^{2+}}$	8.3±0.4	4.9±0.1	8.1±0.4

F_{Pb}^{2+}	4.7±0.3	3.2±0.3	4.3±0.3
F_{Cd}^{2+}	0.0	0.0	0.0
F_{Co}^{2+}	0.0	0.0	0.0
F_{Zn}^{2+}/F_{Cu}^{2+}	3.0	3.8	8.9
F_{Zn}^{2+}/F_{Pb}^{2+}	5.3	5.9	16.7

This obtained results reveal clearly the facilitated diffusion of the three metal cations Zn^{2+}, Cu^{2+} and Pb^{2+}. As observed for the liquid membrane M_L, the individual transport experiments (Fig. 7A) show that the Zn^{2+} cation is transported through the M_s membrane more efficiently than the other metals, with a diffusion flux of 24.7×10^{-3} mol.h^{-1}.m^{-2}. The diffusion fluxes of Cu^{2+} and Pb^{2+}, are found to be 8.3×10^{-3} and 4.7×10^{-3}, respectively, while the Cd^{2+} and Co^{2+} cations are not transferred through the M_s membrane.

From Fig. 7B, the competitive transport data of the five metals agrees with the results obtained for the individual transport. Similar to the **M**$_L$ liquid membrane, the ionophore properties of the carrier were also conserved inside the solid membrane **M**$_S$. Compared to the individual transport, although a decrease in the diffusion flux was observed, the obtained results show a remarkable selectivity of the **M**$_S$ membrane for the Zn^{2+} transport. Its flux was 18.8×10^{-3} mol.h^{-1}.m^{-2}, with $F_{Zn}^{2+}/F_{Cu}^{2+}$and F_{Zn}^{2+}/F_{Pb}^{2+}selectivities of 3.8 and 5.9, respectively.

To further improve the diffusion rates, we studied the competitive transport of the five metals against a proton countercurrent, replacing the receiving phase containing pure water with a solution of nitric acid at a concentration of 2 10^{-3} M. This maintains the electroneutrality of both phases since their nitrate concentrations are equal. The results are plotted in Fig. 7C. The measured metal cation concentrations show a significant improvement in the transport of Zn^{2+} in terms of flux diffusion and selectivity. In fact, its diffusion flux is multiplied by a factor of 3.85, reaching the value of 72.5×10^{-3} mol.h^{-1}.m^{-2}.

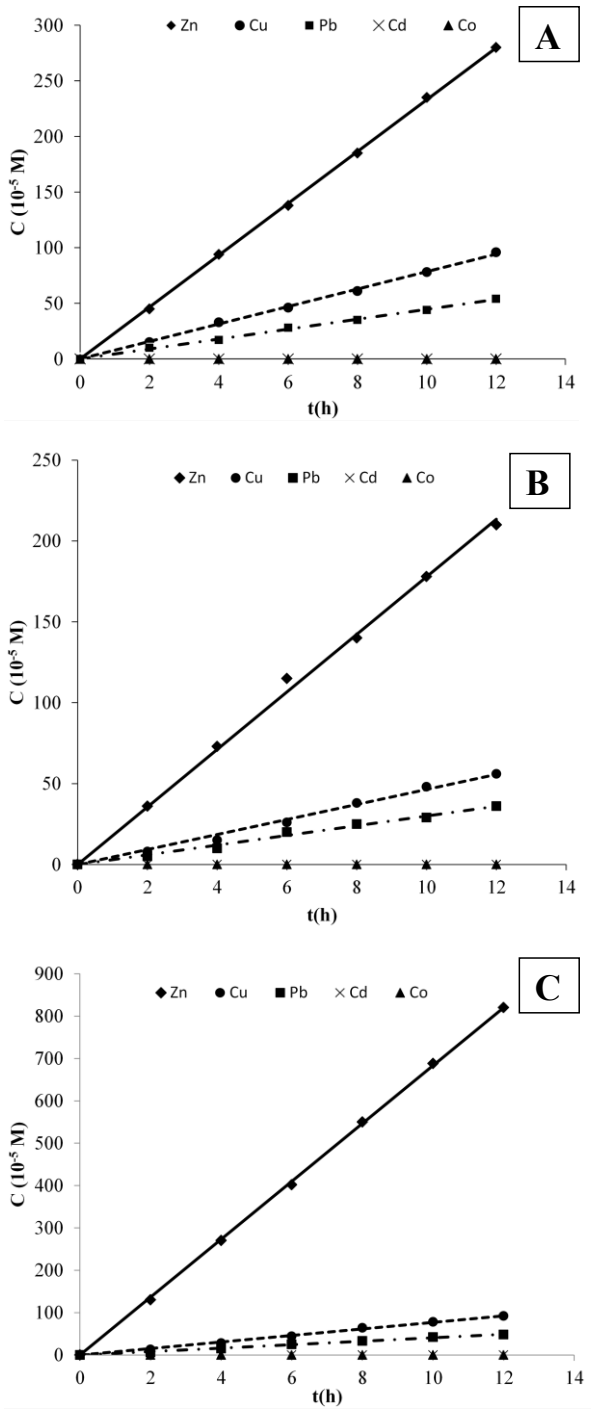

Fig. 7. Individual transport (A), competitive transport (B) and competitive transport against proton current (C) of transition cations through the $\mathbf{M_s}$ solid membrane and temporal evolution of the concentrations of each ion in the reception phase.

Finally, the probability of possible formation of Zn^{2+}-carrier complex was checked within the solid membrane $\mathbf{M_S}$ at the end of the performed individual transport experiment. This was

carried out by inserting the membrane between two compartments where the source was a solution of HNO_3(10^{-1}M) and the reception compartment contains only deionized water. After 12 h test, an insignificant quantity of Zn^{2+} was observed in the receiving phase. This phenomenon could be the result of weak stability of the "Zn^{2+}-carrier" complex as evidenced by the extraction and back-extraction studies. Hence, the blockage of Zn^{2+} cation in the membrane channels is prevented ensuring the stability of the diffusion flux and selectivity.

3.5 *Membrane stability*

The stability of a membrane is based in its ability to preserve its separation performance over time, which determines its durability. In this context, we studied the stability of both liquid and solid membranes by conducting eight cycles of the competitive transport test. This was conducted by renewing both the source and receiving aqueous solutions in each cycle. The results are displayed in Fig. 8 for both liquid and solid membranes. Fig. 8A shows a drastic decrease of the diffusion flux of metal cations through the liquid membrane ($\mathbf{M_L}$) from the third cycle. In fact, the diffusion flux of Zn^{2+} loses half of its value at the eighth cycle, diminishing the performance of this membrane. This instability may be due to the loss of the transporter in the aqueous phases, the formation of an emulsion at the membrane interfaces [29], or to the evaporation of the solvent from the organic phase [30]. On the contrary, as can be seen in Fig. 8B, the flux diffusion of cations through the solid membranes (**Ms**) remains practically constant, and consequently the selectivity of this membrane was maintained stable.

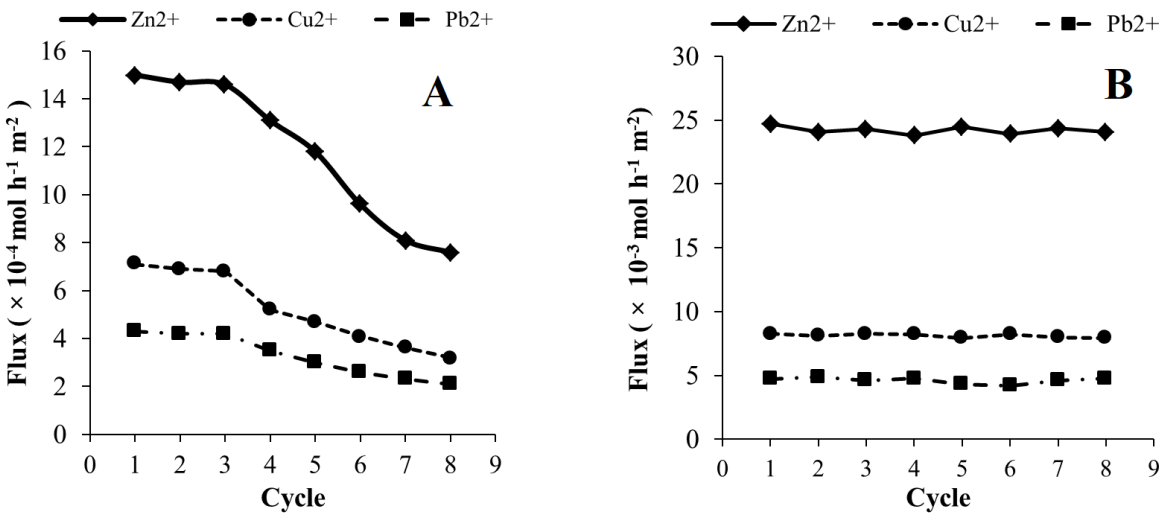

Fig. 8. Flux diffusion of transition metal cations in each cycle for both **M**$_L$ (**A**) and **M**$_S$ (**B**) membranes.

3.6 *Comparative studies of the membranes* M_L *and* M_S*, and other studies*

Careful examination of the diffusion flux of Zn^{2+} cation in the competitive transport reveals that value observed for the solid membrane **M**$_S$ is 31 times higher than that of the liquid membrane **M**$_L$ incorporating the same carrier. The diffusion fluxes of Cu^{2+} and Pb^{2+} are also greater for the **M**$_S$ membrane. Compared to the **M**$_L$ membrane, these were multiplied by a factor of 29 and 40 for Cu^{2+} and Pb^{2+}, respectively. However, although the diffusion fluxes are higher for the solid membrane **M**$_S$, it appears that this membrane is less selective. In fact, the $S_{Zn^{2+}/Cu^{2+}}$ selectivity remains practically constant while the $S_{Zn^{2+}/Pb^{2+}}$ selectivity decreased from 7.6 to 5.9. Furthermore, the stability of the **M**$_S$ membrane is better because its performance varies slightly. This may be attributed partly to the different transport mechanism of the studied cations through the liquid **M**$_L$ and solid **M**$_S$ membranes. The transport of the selected cations through the liquid membrane from the feeding compartment to the receiving one is conducted by diffusion of the carrier through the membrane [31], while the transport through the solid membrane is carried out according to the fixed-site jumping mechanism [32] due to the immobilization of pyrazole-tetrazole transporter onto the crosslinked poly(styrene-co-

methacrylate) copolymer. The above findings are consistent with the studies reported by Scindia et al. [33] who compared the ability to transport Cr(VI) ions by a supported liquid membrane and a solid polymeric membrane. The solid membrane maintained its transport stability for 3 months, while the liquid membrane was operated only for 7 days. These results demonstrated the effectiveness of the transporter grafting on the membrane stability. In fact, the transporter is chemically bound in the polymer matrix, preventing its dissolution in the surrounding aqueous phases.

In the open literature, several selective membranes were proposed for the transport of zinc cation. Nevertheless, the difference of the performed experimental conditions makes the comparison of their performances relative. Table 7 summarizes the values of the diffusion flux of Zn^{2+} cation across the membranes $\mathbf{M_L}$ and $\mathbf{M_S}$ together with those reported for other membranes [34-38]. The comparison between these values clearly reveals that the polymer inclusion membrane involving the diethyldithiocarbamate as carrier (**M2**) exhibits an extremely high diffusion flux (i.e., at least two order of magnitude greater than that of the other membranes). The diffusion flux of Zn^{2+} of the **Ms** membrane prepared in this study is significantly greater than those of the **M1**, **M3**, **M4** membranes. It is however important to point out that the high diffusion flux of the membrane **M2** resulted from the transport experiment against proton current, which tends to increase significantly the diffusion flux , as observed for the **Ms** membrane for which we have clearly shown that the transport flux Zn^{2+} value is 3.8 times higher ($7.25\ 10^{-2}$ mol h^{-1} m^{-2}) at the competitive transport against proton current. In addition, its $S_{Zn^{2+}/Cu^{2+}}$ selectivity, 8.9, is significantly better than the corresponding value ($S_{Zn^{2+}/Cu^{2+}} = 3.2$) observed for the **M2** membrane. Although the **M5** polymer inclusion membrane displays higher diffusion flux ($17.02\ 10^{-2}$ mol.h^{-1}.m^{-2}) than the **Ms** membrane ($1.81\ 10^{-2}$ mol h^{-1} m^{-2}), this flux decreases to $4.86\ 10^{-3}$ mol h^{-1} m^{-2} after only five cycles.

371 **Table 7.** Performance of the $\mathbf{M_L}$ and $\mathbf{M_S}$ membranes developed in this study and their
372 comparison to other membranes reported in the literature.

Membrane*	Flux / mol.h^{-1}.m^{-2}	[Zn^{2+}]$_0$ / mol.L^{-1}	Anion	T / °C	Reference
M1	1.58 10^{-3}	5 10^{-4}	SO_4^{2-}	25	[34]
M2	1.92	10^{-3}	NO_3^-	25	[35]
M3	3,45 10^{-5}	10^{-2}	Cl^-	20	[36]
M4	8.64 10^{-7}	18.5 10^{-4}	Cl^-	25	[37]
M5	17.02 10^{-2}	3.1 10^{-4}	SO_4^{2-}	---	[38]
$\mathbf{M_L}$	6.1 10^{-4}	2 10^{-4}	NO_3^-	25	This work
$\mathbf{M_S}$	1.81 10^{-2}	2 10^{-4}	NO_3^-	25	This work

373 ***M1** = Cellulose triacetate membrane. Plasticizer, o-Nitrophenyl phenyl ether Tris(2-n-butoxyethyl)phosphate/ :
374 bathophenanthroline; **M2** = Polymer inclusion membrane: sodium diethyldithiocarbamate; **M3** = Polymer
375 inclusion membrane: di(2-ethylhexyl)phosphoric acid; **M4** = Supported liquid membranes: Tri-n-dodecylamine;
376 **M5** = polymer inclusion membrane: octyl hydroxamic acid and di (2-ethylhexyl) phosphoric acid

377

378 ## 4. Conclusions

379 In this work, liquid $\mathbf{M_L}$ and solid $\mathbf{M_S}$ membranes were evaluated for the selective separation of
380 some bivalent metal ions, including Zn^{2+} cation from aqueous media. The ionophore properties
381 of the carrier inside both membranes were examined via the liquid-liquid extraction process,
382 revealing a good affinity toward the zinc cation. The development of the solid membrane
383 material involved the photopolymerization of a formulation spread onto a PAN support. This
384 formulation included a methacrylic monomer, synthesized through the esterification of the
385 pyrazole-tetrazole alcohol **2** with acryloyl chloride, alongside styrene and 2,2-dimethoxy-2-
386 phenylacetophenone as photoinitiator. The resulting membrane is asymmetric, amorphous and
387 thermally stable up to 330 °C. The transport experiments evidenced that both membranes
388 transport selectively Zn^{2+} with respect to Cu^{2+}, Pb^{2+}, Cd^{2+} and Co^{2+} cations. The achieved

diffusion fluxes were 1.5 10^{-3} and 6.1 10^{-4} $mol.h^{-1}.m^{-2}$ for the $\mathbf{M_L}$ and $\mathbf{M_S}$ membranes, respectively. Although the $\mathbf{M_S}$ membrane shows the best Zn^{2+} diffusion flux together with a high stability (8 cycles), its selectivity was found to be lower than that of the liquid membrane $\mathbf{M_L}$. The present findings suggest that the solid membrane $\mathbf{M_S}$ could be a good membrane candidate for the selective separation of zinc cation.

Data availability

Data will be made available on request.

Conflict of interest

The authors declare that they have no known competing financial interests or personal relationships that could have appeared to influence the work reported in this paper.

CRediT authorship contribution statement

Tarik Harit: Investigation, Writing – original draft, Methodology. **Mounir Cherfi**: Investigation, Methodology, Formal analysis, Visualization. **Smail Triki**: Formal analysis, Visualization, Writing – review & editing **M. Khayet:** Writing – review & editing. **Fouad Malek**: Writing – review & editing, Supervision, administration.

Acknowledgements

This work was supported by the University Mohamed 1st, the University of Brest and CNRS (Centre National de Recherche Scientifique).

Supplementary materials

Supplementary material associated with this article can be found, in the online version, at ..

References

[1] C. T. Chasapis, P. S. A. Ntoupa, C. A. Spiliopoulou, M. E. Stefanidou, Recent aspects of the effects of zinc on human health, Arch. Toxicol. 94 (2020) 1443-1460, https://doi.org/10.1007/s00204-020-02702-9.

[2] M. Ijaz, M. Zafar, A. Islam, S. Afsheen, T. Iqbal, A review on antibacterial properties of biologically synthesized zinc oxide nanostructures, J. Inorg. Organomet. Polym. Mater. 30 (2020) 2815-2826, https://doi.org/10.1007/s10904-020-01603-9.

[3] M. Pellei, F. Del Bello, M. Porchia, C. Santini, Zinc coordination complexes as anticancer agents, Coord. Chem. Rev. 445 (2021) 214088, https://doi.org/10.1016/j.ccr.2021.214088.

[4] M. S. Nasrollahzadeh, R. Ghodsi, F. Hadizadeh, M. Maleki, M. Mashreghi, D. Poy, Zinc oxide nanoparticles as a potential agent for antiviral drug delivery development: A systematic literature review, Curr. Nanosci. 18 (2022) 147-153, https://doi.org/10.2174/1573413717666210618103632.

[5] Z. Xie, H. Wu, J. Zhao, Multifunctional roles of zinc in Alzheimer's disease, Neurotoxicology, 80 (2020) 112-123, https://doi.org/10.1016/j.neuro.2020.07.003.

[6] D. D. N. Marreiro, K. J. C. Cruz, A. D. Oliveira, J. B. S. Morais, B. J. E. S. A, Freistas, S. R. D. S. Melo, L, R, D, Santos, B. E. P. Cardoso, T. M. D. S. Dias, Antiviral and immunological activity of zinc and possible role in COVID-19. Br. J. Nutr. 127 (2021) 1172-1179, https://doi.org/10.1017/S0007114521002099.

[7] A. Pal, R. Squitti, M. Picozza, A. Pawar, M. Rongioletti, A. K. Dutta, S. Sahoo, K. Goswami, P. Sharma, R. Prasad, Zinc and COVID-19: basis of current clinical trials, Biol. Trace Elem. Res. 199 (2021) 2882-2892, https://doi.org/10.1007/s12011-020-02437-9.

[8] R. Hou, Y. He, G. Yan, S. Hou, Z. Xie, C. Liao, Zinc enzymes in medicinal chemistry, Eur. J. Med. Chem. 226 (2021) 113877, https://doi.org/10.1016/j.ejmech.2021.113877.

[9] Trading economics, Zinc. https://tradingeconomics.com/commodity/zinc. (accessed 11 March 2003)

[10] J. Hu, Q. Chen, H. Hu, F. Hu, X. Chen, Z. Yin, Extraction enhancement of zinc (II) in ammoniacal media through solvent and synergistic effects: a structural and mechanistic investigation, J. Chem. Eng. 215 (2013) 7-14, https://doi.org/10.1016/j.cej.2012.09.129.

[11] H. Miloudi, A. Tayeb, A. Boos, Z. Mehyou, G. Goetz-Grandmont, A. Bengueddach, Preparation of silicas impregnated with HPBI, HPMSP and DEHPA and their application in the

solid–liquid extraction of Cu (II) and Zn (II), Arab. J. Chem. 10 (2017) S1731-S1740, https://doi.org/10.1016/j.arabjc.2013.06.023.

[12] E. Obotey Ezugbe, S. Rathilal, Membrane technologies in wastewater treatment: a review, Membranes 10 (2020) 89, https://doi.org/10.3390/membranes10050089.

[13] Grand view research: Membrane Separation Technology Market Size, Share & Trends Analysis Report By Technology (Microfiltration, Ultrafiltration, Nanofiltration, Reverse Osmosis), By Application, By Region, And Segment Forecasts, 2022 – 2030, Report ID: GVR-4-68038-503-8, https://www.grandviewresearch.com/industry-analysis/membrane-separation-technology-market, 2022 (accessed 11 March 2003).

[14] T. Harit, F. Malek, New polymeric membrane incorporating a tetrapyrazolic macrocycle for the selective transport of cesium cation, Sep. Purif. Technol. 176 (2017) 8-14, https://doi.org/10.1016/j.seppur.2016.11.051.

[15] F. Malek, M. Persin, A. Ramdani, J. Sarrazin, I. Zidane, Elaboration de nouveaux matériaux membranaires incorporant des macrocycles tetrapyrazoliques. Etude du transport facilité des métaux alcalins Li+, Na+ et K+, New J. Chem. 26 (2002) 876-882, https://doi.org/10.1039/B110617C.

[16]T. Harit, F. Malek, Elaboration of new thin solid membrane bearing a tetrapyrazolic macrocycle for the selective transport of lithium cation, Sep. Purif. Technol. 188 (2017) 394-398, https://doi.org/10.1016/j.seppur.2017.07.060.

[17] F. Malek, A. Ramdani, I. Zidane, S. Radi, Synthesis and transport abilities of new membrane materials incorporating mono-and bi-pyrazolic compounds, Eur. Polym. J. 41 (2005) 817-821, https://doi.org/10.1016/j.eurpolymj.2004.11.003.

[18] Zhao, W., Liu, L., Wang, L., & Li, N. (2016). Functionalization of polyacrylonitrile with tetrazole groups for ultrafiltration membranes. RSC advances, 6(76), 72133-72140. https://doi.org/10.1039/C6RA10322G

[19] Fan, W., Peh, S. B., Zhang, Z., Yuan, H., Yang, Z., Wang, Y., ... & Zhao, D. (2021). Tetrazole-functionalized zirconium metal-organic cages for efficient C_2H_2/C_2H_4 and C_2H_2/CO_2 separations. Angewandte Chemie International Edition, 60(32), 17338-17343. https://doi.org/10.1002/anie.202102585

469 [20] M. Cherfi, T. Harit, M. I. Yahyaoui, A. Asehraou, F. Malek, New tetrapodal pyrazole-
470 tetrazole ligands: synthesis, characterization, and evaluation of the antibacterial activity,
471 Polycycl. Aromat. Comp. 43 (2023), 5735-5746,
472 https://doi.org/10.1080/10406638.2022.2105912.

473 [21] M. Cherfi, T. Harit, F. Malek, New macrocycles based on pyrazole-tetrazole subunit:
474 synthesis, characterization and their complexing properties toward heavy metal cations, J. Incl.
475 Phenom. Macrocycl. Chem. 103(2023) 63-70, https://doi.org/10.1007/s10847-023-01177-2.

476 [22] M. Cherfi, T. Harit, I. Dib, M. I. Yahyaoui, A. Asehraou, A. Yahyi, A. Ziyyat, F. Malek,
477 Pyrazole-tetrazole hybrid compounds: Synthesis, characterization and their biological
478 activities, Chem. Data Collect. 45 (2023) 101026, https://doi.org/10.1016/j.cdc.2023.101026.

479 [23] E. L. Cussler, R. Aris, A. Bhown, On the limits of facilitated diffusion, J. Membr. Sci. 43
480 (1989) 149-164, https://doi.org/10.1016/S0376-7388(00)85094-2.

481 [24] N. Scharnagl, H. Buschatz, Polyacrylonitrile (PAN) membranes for ultra-and
482 microfiltration, Desalination 139 (2001) 191-198, https://doi.org/10.1016/S0011-
483 9164(01)00310-1.

484 [25] T. A. Adegbola, O. Agboola, O. S. I. Fayomi, Review of polyacrylonitrile blends and
485 application in manufacturing technology: recycling and environmental impact. Results Eng. 7
486 (2020) 100144. https://doi.org/10.1016/j.rineng.2020.100144.

487 [26] A. Gherrou, H. Kerdjoudj, R. Molinari, P. Seta, E. Drioli, Fixed sites plasticized cellulose
488 triacetate membranes containing crown ethers for silver (I), copper (II) and gold (III) ions
489 transport, J. Membr. Sci. 228 (2004) 149-157, https://doi.org/10.1016/j.memsci.2003.10.003.

490 [27] R. F. Ribeiro, L. C. Pardini, N. P. Alves, C. A. R. Brito Júnior, Thermal Stabilization study
491 of polyacrylonitrile fiber obtained by extrusion, Polímeros 25 (2015) 523-530,
492 https://doi.org/10.1590/0104-1428.1938.

493 [28] W. X. Zhang, Y. Z. Wang, C. F. Sun, Characterization on oxidative stabilization of
494 polyacrylonitrile nanofibers prepared by electrospinning, J. Polym. Res. 14 (2007) 467-474,
495 https://doi.org/10.1007/s10965-007-9130-x.

[29] L. D. Nghiem, P. Mornane, I. D. Potter, J. M. Perera, R. W. Cattrall, S. D. Kolev, Extraction and transport of metal ions and small organic compounds using polymer inclusion membranes (PIMs), J. Membr. Sci. 281 (2006) 7-41, https://doi.org/10.1016/j.memsci.2006.03.035.

[30] H. Takeuchi, K. Takahashi, W. Goto, Some observations on the stability of supported liquid membranes, J. Membr. Sci. 34 (1987) 19-31, https://doi.org/10.1016/S0376-7388(00)80018-6.

[31] J. M. Lehn, La chimie supramoléculaire : concepts et perspectives, De Boeck Université, 1997.

[32] K. M. White, B. D. Smith, P. J. Duggan, S. L. Sheahan, E. M. Tyndall, Mechanism of facilitated saccharide transport through plasticized cellulose triacetate membranes, J. Membr. Sci. 194 (2001) 165-175, https://doi.org/10.1016/S0376-7388(01)00487-2.

[33] Y. M. Scindia, A. K. Pandey, A. V. R. Reddy, Coupled-diffusion transport of Cr (VI) across anion-exchange membranes prepared by physical and chemical immobilization methods. J. Membr. Sci. 249 (2005) 143-152, https://doi.org/10.1016/j.memsci.2004.10.015.

[34] M. Sugiura, M. Kikkawa, S. Urita, Effect of plasticizer on carrier-mediated transport of zinc ion through cellulose triacetate membranes, Sep. Sci. Technol. 22 (1987) 2263-2268, https://doi.org/10.1080/01496398708068612.

[35] G. Arslana, A. Yılmazb, A. Torc, M. Ersoz, Preparation of polymer inclusion membrane with sodium diethyldithiocarbamate as a carrier reagent for selective transport of zinc ions, Desalin. Water Treat. 75 (2017) 348-356, https://doi.org/10.5004/dwt.2017.20485.

[36] M. Ulewicz, W. Walkowiak, J. Gęga, B. Pośpiech, Zinc (II) selective removal from other transition metal ions by solvent extraction and transport through polymer inclusion membranes with D2EHPA, Ars Separatoria Acta, (2003) 47-5.

[37] H. Ur Rehman, G. Akhtar, H. Ur Rashid, N. Ali, I. Ahmad, S. Ur Rehman, K. Khan, M. Arshad, Transport of Zn (II) by TDDA-polypropylene supported liquid membranes and recovery from waste discharge liquor of galvanizing plant of Zn (II). J. Chem. 2017 (2017) 1-9, https://doi.org/10.1155/2017/7569354.

523 [38] C. Li, Y. Jia, X. Lu, H. Chen, Transport of Zn (II) through matrix enhanced polymer
524 inclusion membrane containing OHA and D2EHPA, Chem. Eng. J. 452 (2023) 139288,
525 https://doi.org/10.1016/j.cej.2022.139288.

526